Inorg. Chem. **2008**, *47*, 8294−8305

Electrochemical and Complexation Behavior of Neptunium in Aqueous Perchlorate and Nitrate Solutions

Atsushi Ikeda-Ohno,*,†,‡ Christoph Hennig,*,† André Rossberg,† Harald Funke,† Andreas C. Scheinost,† Gert Bernhard,† and Tsuyoshi Yaita‡

Institute of Radiochemistry, Forschungszentrum Dresden-Rossendorf, P.O. Box 510119, 01314 Dresden, Germany, and Japan Atomic Energy Agency (JAEA) (Spring-8), Kouto 1-1-1, Sayo-cho, Sayo-gun, Hyogo 679-5148, Japan

Received May 18, 2008

Electrochemical and complexation properties of neptunium (Np) are investigated in aqueous perchlorate and nitrate solutions by means of cyclic voltammetry, bulk electrolysis, UV−visible absorption, and Np L_{III}-edge X-ray absorption spectroscopies. The redox reactions of Np^{III}/Np^{IV} and Np^{V}/Np^{VI} couples are reversible or quasi-reversible, while the electrochemical reaction between $Np^{III/IV}$ and $Np^{V/VI}$ is irreversible because they undergo structural rearrangement from spherical coordinating ions (Np^{3+} and Np^{4+}) to transdioxoneptunyl ions (NpO_2^{n+}, $n = 1$ for Np^{V} and 2 for Np^{VI}). The redox reaction of the Np^{V}/Np^{VI} couple involves no structural rearrangement on their equatorial planes in acidic perchlorate and nitrate solutions. A detailed analysis on extended X-ray absorption fine structure (EXAFS) spectra suggests that Np^{IV} forms a decaaquo complex of $[Np(H_2O)_{10}]^{4+}$ in 1.0 M $HClO_4$, while Np^{V} and Np^{VI} exist dominantly as pentaaquoneptunyl complexes, $[NpO_2(H_2O)_5]^{n+}$ ($n = 1$ for Np^{V} and 2 for Np^{VI}). A systematic change is observed on the Fourier transforms of the EXAFS spectra for all of the Np oxidation states as the nitrate concentration is increased in the sample, revealing that the hydrate water molecules are replaced by bidentate-coordinating nitrate ions on the primary coordination sphere of Np.

Introduction

The chemistry of actinides (An) in aqueous solution is fundamental to the nuclear fuel industry. The reprocessing process of spent nuclear fuels, such as PUREX,[1] involves the use of aqueous acidic solutions in order to dissolve the fuels for the separation of fissile nuclides of uranium (U) and plutonium (Pu) from other An and fission products by solvent extraction. Furthermore, the assessment of environmental impact on the geological disposal of radioactive wastes requires vast information about the chemical properties of An in a natural aquatic environment for predicting their migration behavior in an aquifer.[2] Hence, sustaining and developing the industrial fields relevant to nuclear fuels require extensive information about the basic chemistry of An in aqueous solutions, such as solubility, speciation distribution, redox character, or complexation and coordination behavior.

Neptunium (Np) is one of the artificial elements produced in nuclear reactors. It is located between U and Pu on the periodic table, suggesting that its chemical properties are qualitatively similar to those of U and Pu.[3] Because of this chemical similarity to recyclable U and Pu, as well as its considerable content in spent nuclear fuels, the behavior of Np is one of the most important issues to be considered in the fuel reprocessing process. Besides, the long half-lives of Np nuclides [e.g., $T_{1/2}(^{237}Np) = 2.14 \times 10^6$ years] and their high solubility under environmentally relevant conditions make them problematic on the long-term repository of

* To whom correspondence should be addressed. E-mail: a.ikeda-ohno@spring8.or.jp (A.I.-O.), hennig@esrf.fr (C.H.).
† Institute of Radiochemistry.
‡ Japan Atomic Energy Agency, Synchrotron Radiation Research Center.

(1) (a) Long, J. T. *Engineering for Nuclear Fuel Reprocessing*; American Nuclear Society: La Grange Park, IL, 1978. (b) Benedict, M.; Pigford, T. H.; Levi, H. W. *Nuclear Chemical Engineering*, 2nd ed.; McGraw-Hill: New York, 1981.
(2) (a) Chapman, N. A.; McKinley, I. G.; Hill, M. D. *The Geological Disposal of Nuclear Waste*; John Wiley & Sons: Chichester, Great Britain, 1987. (b) Nash, K. L.; Cleveland, J. M.; Rees, T. F. *J. Environ. Radioact.* **1988**, *7*, 131–157. (c) Dozol, M.; Hagemann, R. *Pure Appl. Chem.* **1993**, *65*, 1081–1102.
(3) (a) Choppin, G. R. *Radiochim. Acta* **1983**, *32*, 45–53. (b) Choppin, G. R.; Nash, K. L. *Radiochim. Acta* **1995**, *70/71*, 225–236. (c) Silva, R. J.; Nitsche, H. *Radiochim. Acta* **1997**, *70/71*, 377–396.

10.1021/ic8009095 CCC: $40.75
Published on Web 08/13/2008

radioactive wastes.[4] Accordingly, for the last several decades, Np chemistry has received a variety of experimental studies to understand the chemical properties of Np in aqueous solutions, including thermodynamic,[5,6] electrochemical,[7,8] and spectroscopic properties,[9,10] and the structural arrangement of complexes.[11] Furthermore, in recent years, a theoretical approach has become powerful in gaining insight into the detailed physical and chemical properties of Np, simulating chemical systems that are experimentally difficult to investigate, and supporting the experimental data.[12,13]

One of the peculiarities of Np chemistry is its variety of possible oxidation states. It is known that Np can possess five different oxidation states from III to VII in aqueous solution and, furthermore, its coordination environment depends on the oxidation state. The Np species in tri- and tetravalent states form spherically coordinated Np^{3+} and Np^{4+} cations in solution, whereas those in penta- and hexavalent states exist as linearly arranged *trans*-dioxo cations, namely, neptunyl ions (NpO_2^{n+}, $n = 1$ for Np^{V} and 2 for Np^{VI}). Besides, the heptavalent state of Np exhibits an unusual tetraoxo coordination geometry of NpO_4^- in a highly basic solution.[11e,f] The unit structure of the Np ion governs its complexation property, which plays an important role in determining the behavior of Np in actual chemical processes. Therefore, detailed knowledge about the Np coordination environment in different oxidation states is indispensable both for basic and for applied research fields relevant to Np.

To date, structural investigation of aqueous Np species with different oxidation states has been reported for acidic solutions of HCl[11b] and diluted HNO_3[11d] and in a basic NaOH solution.[11e] However, in these precedent studies, the solution compositions have been modified for each oxidation state to avoid the reoxidation/rereduction of prepared Np species, with the result that the structural comparison between different oxidation states has not been achieved under identical solution conditions. The remarkable study by Antonio and his co-workers using the in situ spectroelectrochemical cell[11g] is the only example that has performed a systematic investigation on the structure of Np species as a function of the oxidation state under the same solution conditions. They have acquired the structural information for the hydrate species of Np^{III}, Np^{IV}, Np^{V}, and Np^{VI} in a 1.0 M $HClO_4$ solution by means of extended X-ray absorption fine structure (EXAFS) spectroscopy. However, the structural parameters obtained in this study contain relatively large errors (interatomic distances, $R \pm 0.02-0.03$ Å, and coordination numbers, $N \pm 10-20\%$) because of the low Np concentration in the sample. Therefore, further investigation is still required even for the simplest aqueous species of neptunium hydrates not only to understand their detailed coordination environment but also to supply more accurate reference values to the related theoretical calculations. Moreover, concerning other aqueous solution systems, no systematic study has been carried out on the coordination chemistry of Np as a function of the oxidation state. These facts motivate us to perform the present systematic study on the coordination behavior of Np with different oxidation states in aqueous solution systems. That is, we investigate the electrochemical behavior of Np in aqueous perchlorate and nitrate solutions to understand the redox properties of aqueous Np species and to define the appropriate conditions for stabilizing the Np species at each oxidation state. The structural arrangements of the prepared Np species are identified by X-ray absorption spectroscopy (XAS) and the structural variation consequent upon a change in the oxidation

(4) (a) Hursthouse, A. S.; Baxter, M. S.; Livens, F. R.; Duncan, H. J. *J. Environ. Radioact.* **1991**, *14*, 147–174. (b) Viswanathan, H. S.; Robinson, B. A.; Valocchi, A. J.; Triay, I. R. *J. Hydrol.* **1998**, *209*, 251–280. (c) Kaszuba, J. P.; Runde, W. H. *Environ. Sci. Technol.* **1999**, *33*, 4427–4433.

(5) Lemire, R. J.; Fuger, J.; Nitsche, H.; Rotter, P.; Rand, M. H.; Rydberg, J.; Spahiu, K.; Sullivan, J. C.; Ullman, W. J.; Vitorge, P.; Wanner, H. *Chemical Thermodynamics of Neptunium and Plutonium*; OECD-NEA, Data Bank Issy-les-Moulineaux Eds.; OECD-NEA: Amsterdam, The Netherlands, 2001 (2003 updated).

(6) (a) Lahr, H.; Knoch, W. *Radiochim. Acta* **1970**, *13*, 1–5. (b) Chang, C.-T.; Liaw, C.-F. *J. Inorg. Nucl. Chem.* **1971**, *33*, 2623–2630. (c) Danesi, P. R.; Chiarizia, R.; Scibona, G.; D'Alessandro, G. *J. Inorg. Nucl. Chem.* **1971**, *33*, 3503–3510. (d) Moskvin, A. I. *Russ. J. Inorg. Chem.* **1971**, *16*, 405–408. (e) Spahiu, K.; Puigdomenech, I. *Radiochim. Acta* **1998**, *82*, 413–419. (f) Kappenstein-Grégoire, A. C.; Moisy, P.; Cote, G.; Blanc, P. *Radiochim. Acta* **2003**, *91*, 371–378.

(7) (a) Hindman, J. C.; Cohen, D. *J. Am. Chem. Soc.* **1950**, *72*, 953–956. (b) Cohen, D.; Hindman, J. C. *J. Am. Chem. Soc.* **1952**, *74*, 4679–4682. (c) Cohen, D.; Hindman, J. C. *J. Am. Chem. Soc.* **1952**, *74*, 4682–4685. (d) Kihara, S.; Yoshida, Z.; Aoyagi, H.; Maeda, K.; Shirai, O.; Kitatsuji, Y.; Yoshida, Y. *Pure Appl. Chem.* **1999**, *71*, 1771–1807. (e) Aoyagi, H.; Kitatsuji, Y.; Yoshida, Z.; Kihara, S. *Anal. Chim. Acta* **2005**, *538*, 283–289.

(8) (a) Plock, C. E. *J. Electroanal. Chem.* **1968**, *18*, 289–293. (b) Casadio, S.; Orlandini, F. *J. Electroanal. Chem.* **1971**, *33*, 212–215. (c) Kim, S.-Y.; Asakura, T.; Morita, Y.; Uchiyama, G.; Ikeda, Y. *J. Radioanal. Nucl. Chem.* **2004**, *262*, 311–315. (d) Yamamura, T.; Watanabe, N.; Yano, T.; Shiokawa, Y. *J. Electrochem. Soc.* **2005**, *152*, A830−A836. (e) Kim, S.-Y.; Asakura, T.; Morita, Y. *Radiochim. Acta* **2005**, *93*, 767–770.

(9) (a) Hindman, J. C.; Magnusson, L. B.; LaChapelle, T. J. *J. Am. Chem. Soc.* **1949**, *71*, 687–693. (b) Sjoblom, R.; Hindman, J. C. *J. Am. Chem. Soc.* **1951**, *73*, 1744–1751. (c) Cohen, D. *Inorg. Nucl. Chem. Lett.* **1976**, *12*, 635–637.

(10) (a) Friedman, H. A.; Toth, L. M. *J. Inorg. Nucl. Chem.* **1980**, *42*, 1347–1349. (b) Denning, R. G.; Norris, J. O. W.; Brown, D. *Mol. Phys.* **1982**, *46*, 287–323.

(11) (a) Combes, J.-M.; Chisholm-Brause, C. J.; Brown, G. E., Jr.; Parks, G. A.; Conradson, S. D.; Eller, P. G.; Trlay, I. R.; Hobert, D. E.; Meljer, A. *Environ. Sci. Technol.* **1992**, *26*, 376–382. (b) Allen, P. G.; Bucher, J. J.; Shuh, D. K.; Edelstein, N. M.; Reich, T. *Inorg. Chem.* **1997**, *36*, 4676–4683. (c) Clark, D. L.; Conradson, S. D.; Neu, M. P.; Palmer, P. D.; Runde, W.; Tait, C. D. *J. Am. Chem. Soc.* **1997**, *119*, 5259–5260. (d) Reich, T.; Bernhard, G.; Geipel, G.; Funke, H.; Hennig, C.; Rossberg, A.; Matz, W.; Schell, N.; Nitsche, H. *Radiochim. Acta* **2000**, *88*, 633–637. (e) Williams, C. W.; Blaudeau, J.-P.; Sullivan, J. C.; Antonio, M. P.; Bursten, B.; Soderholm, L. *J. Am. Chem. Soc.* **2001**, *123*, 4346–4347. (f) Bolvin, H.; Wahlgren, U.; Moll, H.; Reich, T.; Geipel, G.; Fanghänel, T.; Grenthe, I. *J. Phys. Chem. A* **2001**, *105*, 11441–11445. (g) Antonio, M. R.; Soderholm, L.; Williams, C. W.; Blaudeau, J.-P.; Bursten, B. E. *Radiochim. Acta* **2001**, *89*, 17–25. (h) Denecke, M. A.; Dardenne, K.; Marquardt, C. M. *Talanta* **2005**, *65*, 1008–1014. (i) Hennig, C. *Phys. Rev. B* **2007**, *75*, 035120. (j) Skanthakumar, S.; Antonio, M. R.; Soderholm, L. *Inorg. Chem.* **2008**, *47*, 4591–4595.

(12) (a) Pyykkö, P. *Inorg. Chim. Acta* **1987**, *139*, 243–245. (b) Pepper, M.; Bursten, B. E. *Chem. Rev.* **1991**, *91*, 719–741. (c) Schreckenbach, G.; Hay, P. J.; Martin, R. L. *J. Comput. Chem.* **1999**, *20*, 70–90. (d) Vallet, V.; Macak, P.; Wahlgren, U.; Grenthe, I. *Theor. Chem. Acc.* **2006**, *115*, 145–160.

(13) (a) Matsika, S.; Pitzer, R. M. *J. Phys. Chem. A* **2000**, *104*, 4064–4068. (b) Hay, P. J.; Martin, R. L.; Schreckenbach, G. *J. Phys. Chem. A* **2000**, *104*, 6259–6270. (c) Bolvin, H.; Wahlgren, U.; Gropen, O.; Marsden, C. *J. Phys. Chem. A* **2001**, *105*, 10570–10576. (d) Cao, Z.; Balasubramanian, K. *J. Chem. Phys.* **2005**, *123*, 114309. (e) Steele, H.; Taylor, R. J. *Inorg. Chem.* **2007**, *46*, 6311–6318. (f) Wiebke, J.; Moritz, A.; Cao, X.; Dolg, M. *Phys. Chem. Chem. Phys.* **2007**, *9*, 459–465.

Table 1. Summary of XAS Samples

ID	system	oxidation state of Np	[Np]/M	medium	preparation[a]
1	perchlorate	IV	0.04	1.0 M $HClO_4$	reduction of Np^V at −0.3 V
2		V	0.04	1.0 M $HClO_4$	reduction of Np^{VI} at 0.2 V
3		VI	0.04	1.0 M $HClO_4$	dissolution of the dried Np stock solution
4	nitrate	IV	0.04	1.0 M HNO_3/4.0 M NH_4NO_3	reduction of Np^V at −0.3 V
5		V	0.04	1.0 M HNO_3/4.0 M NH_4NO_3	reduction of Np^{VI} at 0.2 V
6		VI	0.04	1.0 M HNO_3/4.0 M NH_4NO_3	dissolution of the dried Np stock solution
7		IV	0.04	4.4 M HNO_3/6.0 M NH_4NO_3	reduction of Np^V at −0.3 V
8		VI	0.04	4.4 M HNO_3/6.0 M NH_4NO_3	dissolution of the dried Np stock solution
9		VI	0.04	14.5 M HNO_3	dissolution of the dried Np stock solution

[a] Potentials are referred to Ag/AgCl.

state is discussed. As mentioned above, the Np species formed in an aqueous perchlorate solution are simple hydrate complexes because perchlorate ions hardly bind to the primary coordination sphere of An ions in aqueous solution.[11g,14] Therefore, the perchlorate solution was chosen as a noncomplexing system, in order to investigate the most basic aqueous species of hydrate complexes. On the other hand, as mentioned above, the nitrate solution is essential for nuclear fuel reprocessing. The purpose of this study is to reveal the fundamental redox and coordination properties of Np in aqueous solutions. The obtained results will be informative not only for the aqueous An chemistry but also for the basic and applied research fields relevant to the nuclear fuel industry.

Experimental Section

Caution! *^{237}Np is a radioactive isotope ($T_{1/2} = 2.14 \times 10^6$ years) and an α-emitter. It should be handled in dedicated facilities with appropriate equipment for radioactive materials to avoid health risks caused by radiation exposure.*

Sample Preparation. Neptunium (^{237}Np) dioxide was obtained from CEA-Marcoule, France. NpO_2 was dissolved in 14.5 M HNO_3 at ∼283 K, giving a pale-ocher solution. The solution was then evaporated to dryness by heating, and the dried material was dissolved in 1.0 M $HClO_4$. This evaporation/dissolution process was repeated five times to remove nitrate ions from the solution. The resultant solution was a purple-colored solution and identified as pure Np^{VI} by UV−visible absorption spectroscopy. This solution in 1.0 M $HClO_4$ was used as a Np stock solution for further sample preparation. The concentration of Np in the stock solution ($[Np^{VI}] = 0.05$ M) was quantified by UV−visible absorption and α/γ spectroscopies. The radiochemical purity of the stock solution was also confirmed by α/γ spectroscopy.

Sample solutions used for electrochemical experiments (i.e., cyclic voltammetry and bulk electrolysis) were prepared by evaporating an appropriate amount of the Np stock solution and dissolving the dried material into a desired composition of an aqueous perchlorate ($HClO_4$) or nitrate (HNO_3/NH_4NO_3) solution. The oxidation states and concentrations of Np in the sample solutions were determined by UV−visible absorption and α/γ spectroscopies. All of the chemicals (except NpO_2) used in this study were reagent grade and supplied by Merck KGaA.

Electrochemical Experiments. Cyclic voltammograms (CVs) of 0.04 M Np^{VI} in aqueous perchlorate and nitrate solutions were recorded at room temperature (approximately 278 K) using an Autolab PGSTAT302 potentiostat/galvanostat (Eco Chemie BV) under a N_2 atmosphere. A three-electrode system consisting of a Pt working electrode (surface area = 2.01 mm^3), a Pt wire counter electrode, and a Ag/AgCl reference electrode (in 3 M NaCl with Vycor glass liquid junction) was employed. CVs of blank solutions were also measured to subtract the influence of the nonfaradic current, such as the charging current or liquid junction potential. Therefore, the CVs presented in this study are all background subtracted. Sample solutions were deoxygenated by bubbling N_2 gas prior to the measurement. Some of the obtained CVs were fitted with the theoretical potential−current curves simulated by the Autolab software package *GPES* based on the finite difference method with the Crank−Nicolson technique,[15] in order to evaluate the kinetic parameters for electrochemical reactions of Np.

On the basis of the obtained CVs, bulk electrolysis was performed in each solution system to adjust the oxidation state of Np in the sample solution. Coulometric electrolysis of 0.04 M Np was carried out with the same potentiostat/galvanostat as that used in cyclic voltammetry by employing the three-electrode system consisting of Pt mesh working and counter electrodes and the Ag/AgCl reference electrode. The oxidation state and concentration of Np in the electrolyzed solutions were confirmed by UV−visible absorption spectroscopy.

XAS Measurements. XAS measurements [X-ray absorption near-edge structure (XANES) and EXAFS] were performed on the Rossendorf beamline (ROBL) BM20[16] at the European Synchrotron Radiation Facility under dedicated ring operating conditions (6 GeV; 130−200 mA). A Si(111) double-crystal monochromator was employed in channel-cut mode to monochromatize a white X-ray from the synchrotron. Np L_{III}-edge absorption spectra were collected in transmission mode by using Ar-filled ionization chambers at ambient temperature and pressure. Energy calibration of the measured spectra was achieved by the simultaneous XAS measurement of the reference Y foil (first inflection point at 17 038 eV). The threshold energy, $E_{k=0}$, of Np L_{III} edge was defined at 17 625 eV, regardless of the oxidation state of Np. Np^{VI} solution samples were prepared by evaporating the Np stock solution and dissolving the dried material into a desired solution. Samples with other Np oxidation states were electrochemically prepared from the corresponding Np^{VI} solutions by bulk electrolysis. The concentration of Np in each sample solution was adjusted to 0.04 M. The detailed compositions of the sample solutions are summarized in Table 1. 0.75 mL of the sample solution was transferred to a triply sealed polystyrene/poly(methyl methacrylate) cuvette (optical path length = 1.0 cm) for XAS measurement. At least two scans were

(14) Sémon, L.; Boehme, C.; Billard, I.; Hennig, C.; Lützenkirchen, K.; Reich, T.; Rossberg, A.; Rossini, I.; Wipff, G. *ChemPhysChem.* **2001**, *2*, 591–598.

(15) (a) Crank, J.; Nicolson, P. *Proc. Cambridge Philos. Soc.* **1947**, *43*, 50–67. (b) Crank, J.; Nicolson, P. *Adv. Comput. Math.* **1996**, *6*, 207–226.

(16) Matz, W.; Schell, N.; Bernhard, G.; Prokert, F.; Reich, T.; Clauβner, J.; Oehme, W.; Schlenk, R.; Dienel, S.; Funke, H.; Eichhorn, F.; Betzl, M.; Pröhl, D.; Strauch, U.; Hüttig, G.; Krug, H.; Neumann, W.; Brendler, V.; Reichel, P.; Denecke, M. A.; Nitsche, H. *J. Synchrotron Radiat.* **1999**, *6*, 1076–1085.

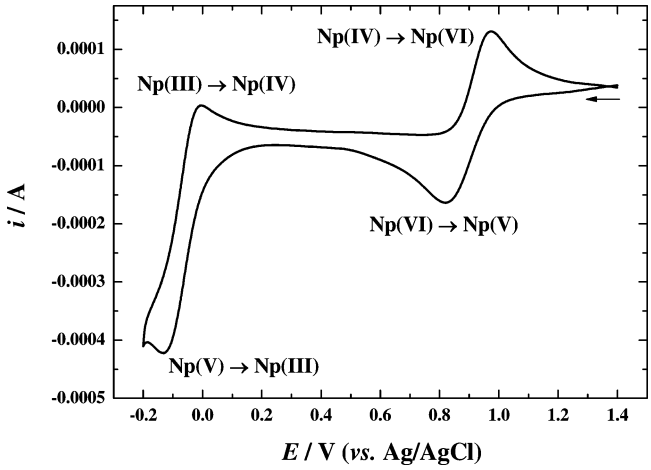

Figure 1. CV of 0.04 M Np^{VI} in 1.0 M $HClO_4$ using a Pt electrode: initial scan direction, anodic (from 1.4 V); scan rate, 100 mV/s.

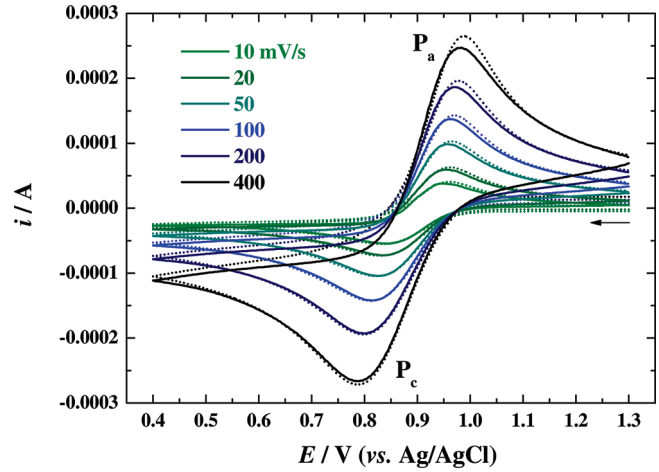

Figure 2. CVs of 0.04 M Np^{VI} in 1.0 M $HClO_4$ using a Pt electrode: —, experimental data; ···, fitting curves; initial scan direction, anodic (from 1.3 V). Fitting curves were simulated by assuming a quasi-reversible system.

performed for each sample, and the spectra were averaged. The obtained spectra were treated according to a standard procedure[17] using the program *WinXAS* (version 3.1).[18] EXAFS curve fitting was achieved in the *R* space (i.e., Fourier-transformed spectra) using theoretical phases and amplitude calculated by *FEFF* 8.20.[19] All of the possible single-scattering (SS) and multiple-scattering (MS) paths were modeled from the crystal structures of the suitable U compounds, $[UO_2(H_2O)_5](ClO_4)_2$[20] and $UO_2(NO_3)_2(H_2O)_2$,[21] by substituting Np for U. The amplitude reduction factor, S_0^2, was fixed at 0.9, and the shifts in the threshold energy, ΔE_0, were constrained to be the same value for all shells.

Results and Discussion

Perchlorate System. Figure 1 shows a CV of Np^{VI} in 1.0 M $HClO_4$ using a Pt working electrode. Two clear peaks observed at +0.7 and −0.1 V (vs Ag/AgCl, the potential values hereafter always refer to Ag/AgCl) on the cathodic scan correspond to the reduction from Np^{VI} to Np^{V} and that from Np^{V} to Np^{III}, respectively, while two anodic peaks observed at −0.05 and +0.95 V result from oxidation from Np^{III} to Np^{IV} and that from Np^{IV} to Np^{VI}, respectively.[7e,22] No further oxidation peak is detected up to 1.7 V, which is the upper limit of the electrochemical window for a Pt electrode in the present $HClO_4$ solution, suggesting that Np^{VI} is not further oxidized to Np^{VII} in a $HClO_4$ solution using a Pt electrode. In fact, the reported Np^{VII} species have been prepared only in strongly basic solutions.[11c,e,f] Additionally, other cyclic voltammetry measurements were carried out at different scan rates with a limited scan range from 1.3 to 0.4 V, in order to evaluate the electrochemical parameters of a Np^{VI}/Np^{V} redox couple. The obtained CVs are given in Figure 2. A pair of redox peaks is clearly observed at each scan rate, and the potential difference between the anodic peak (P_a) and the cathodic peak (P_c), ΔE_p, is slightly increased with an increase in the scan rates, suggesting that the redox reaction of the Np^{VI}/Np^{V} couple is neither a reversible system nor an irreversible one.[23] Therefore, the CV simulations were performed by assuming a quasi-reversible system. The fitting results using the Marquardt nonlinear least-squares method are shown in Figure 2 as dotted lines. The best-fitting curves are simulated with a normalized standard rate constant, k^0_{norm}, of 0.44 ± 0.10,[24] a transfer coefficient, α, of 0.37 ± 0.02,[24] and a formal redox potential, E^0, of 0.90 V. k^0_{norm} is the standard rate constant, which is normalized with respect to the time scale of the experiment, and it is calculated by the following equation:

$$k^0_{norm} = k^0\sqrt{RT/nFVD} \quad (1)$$

where *R*, *T*, *F*, *V*, and *D* are the gas constant (in molar), temperature, Faraday constant, scan rate, and diffusion coefficient, respectively. The value *n* represents a stoichiometric number of electrons involved in an electrochemical reaction, and it should be 1 in the present redox reaction of the Np^{VI}/Np^{V} couple. k^0 is the standard rate constant defined in the following Butler−Volmer equation:[23]

$$i = FAk^0\{C_O \exp[-\alpha F/RT(E-E^0)] - C_R \exp[(1-\alpha)F/RT(E-E^0)]\} \quad (2)$$

where *i*, *A*, and *E* are the peak current, surface area of the electrode, and potential, respectively. C_O and C_R represent the concentrations of the oxidant and reductant at the electrode surface. The obtained E^0 value is in good agreement with those listed in the comprehensive review by Kihara et al. (0.94−0.96 V),[7d] and k^0_{norm} is similar to those evaluated for carbon electrodes in HNO_3 and HCl solutions; k^0_{norm} = 0.35−4.0.[8c−e] This suggests that the obtained CVs and the corresponding simulation results are sufficiently reliable for discussion. The transfer coefficient, α, is a measure of the symmetry of the energy barrier in an electrochemical

(17) Prins, R. ; Koningsberger, D. E. *X-ray Absorption: Principles, Applications, Techniques for EXAFS, SEXAFS, and XANES*; Wiley-Interscience: New York, 1988.
(18) Ressler, T. *J. Synchrotron Radiat.* **1998**, *5*, 118–122.
(19) Ankudinov, A. L.; Ravel, B.; Rehr, J. J.; Conradson, S. D. *Phys. Rev. B* **1998**, *58*, 7565–7576.
(20) Fischer, A. *Z. Anorg. Allgem. Chem.* **2003**, *629*, 1012–1016.
(21) Taylor, J. C.; Mueller, M. H. *Acta Crystallogr.* **1965**, *19*, 536–543.
(22) Li, Y.; Kato, Y.; Yoshida, Z. *Radiochim. Acta* **1993**, *60*, 115–119.
(23) Bard, A. J.; Faulkner, L. R. *Electrochemical Methods—Fundamentals and Applications*, 2nd ed.; John Wiley & Sons: New York, 2001.
(24) These values are the average for the measured scan rates.

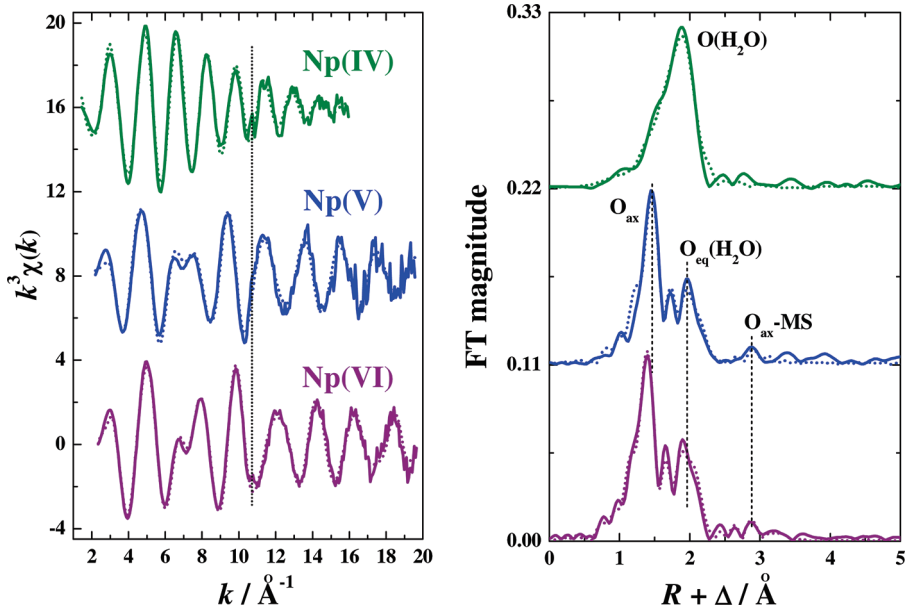

Figure 3. k^3-weighted Np L_{III}-edge EXAFS spectra (left) and their corresponding FTs (right) for Np^{IV}, Np^{V}, and Np^{VI} in 1.0 M $HClO_4$: —, experimental data; •••, theoretical fit; FT range, k = 1.5−16.0 Å^{-1} for Np^{IV} and 2.0−19.5 Å^{-1} for Np^{V} and Np^{VI}, respectively; phase shifts are not corrected on the FTs; the data color reflects the actual color of the sample solutions. The dotted line on the EXAFS spectra represents the [2p4f] double-electron excitation. See the text.

reaction.[23] The obtained value of $\alpha = 0.37$ indicates that the energy barrier for the reductant (i.e., Np^{V} ion) is steeper than that for the oxidant (i.e., Np^{VI} ion),[25] meaning that the reduction from Np^{VI} to Np^{V} is thermodynamically easier than the oxidation from Np^{V} to Np^{VI}. On the other hand, the redox reaction of the Np^{III}/Np^{IV} couple appears to be reversible,[8d] although no detailed analysis was performed for this redox couple in this study.

On the basis of the obtained CVs, the bulk electrolysis was performed to adjust the oxidation state of Np in 1.0 M $HClO_4$. The initial sample solution of 0.04 M Np^{VI} was first reduced at 0.2 V. After the reduction, the color of the solution was changed from purple to blue-green. The UV−visible absorption spectrum of the reduced solution (Figure S3 in the Supporting Information) exhibits sharp peaks at 616, 982, and 1097 nm, corresponding to the previously reported characteristic absorption peaks of Np^{V} in $HClO_4$.[9a,b] The intense absorption peak at 1224 nm, which is observed in the original Np^{VI} solution, is entirely gone after the electrolysis. These facts prove that Np^{VI} in the initial sample solution was completely converted to Np^{V} by the electrolysis and, hence, the obtained blue-green solution was employed as a Np^{V} sample for XAS measurement. Second, the blue-green solution of Np^{V} was further reduced at −0.3 V, producing a dark-brown solution of Np^{III}. This Np^{III} solution is, however, very unstable in air and oxidized to Np^{IV} rapidly.[9a,b] Exposing the Np^{III} solution to air for several hours resulted in a yellow-green solution. This solution is stable in air. The UV−visible absorption spectrum of the resultant solution shows no characteristic peaks of Np^{V} and is consistent with the reported spectrum of Np^{IV} [9a,b] (see Figure S3 in the Supporting Information). Accordingly, the yellow-green solution was used as a Np^{IV} sample for XAS measurement. No Np^{III} sample for XAS measurement was obtained because of the difficulty in keeping Np^{III} stable for a long time at atmospheric conditions. The XAS measurement of Np^{III} species requires specially made in situ spectroelectrochemical cells.[26]

Figure 3 shows the k^3-weighted Np L_{III}-edge EXAFS spectra and the corresponding Fourier transforms (FTs) for Np^{IV}, Np^{V}, and Np^{VI} in 1.0 M $HClO_4$. Clear EXAFS oscillations were observed with fairly high quality from 1.5 to 16.0 Å^{-1} for Np^{IV} and from 2.0 to 19.5 Å^{-1} for Np^{V} and Np^{VI}, respectively. The small and sharp peaks observed at $k \approx 10.7$ Å^{-1} originate from the [2p4f] double-electron excitation.[11i] The spectrum of Np^{IV} is composed of a single EXAFS oscillation, giving only a single peak at $R + \Delta = 1.9$ Å on its FT. The best curve-fitting result for this spectrum calculates the structural parameters of $R = 2.40$ Å and $N = 10.4$, corresponding to the hydrate water molecules in the primary coordination sphere. These values agree with the reported values ($R = 2.40-2.41$ Å and $N = 10-11$),[11b] and they are also quite analogous to those for the uranium(IV) hydrate complex ($R = 2.40-2.41$ Å and $N = 9-11$).[27,28] Np^{V} and Np^{VI} exhibit more intricate oscillation patterns, and their corresponding FTs show several significant peaks. The intense peaks at around $R + \Delta = 1.4$ Å arise from the SS of the axial O atoms (O_{ax}) of Np ions, being a representative

(25) If the intersection of the Gibbs free energy curves for an oxidant and a reductant is symmetrical, α equals to 0.5. The α values below 0.5 mean that the energy curve for the oxidant is gentler than that for the reductant, whereas the α values above 0.5 mean that the energy curve for the oxidant is steeper than that for the reductant.

(26) (a) Soderholm, L.; Antonio, M. R.; Williams, C.; Wasserman, S. R. *Anal. Chem.* **1999**, *71*, 4622–4628. (b) Hennig, C.; Tutschku, J.; Rossberg, A.; Bernhard, G.; Scheinost, A. C. *Inorg. Chem.* **2005**, *44*, 6655–6661.
(27) Moll, H.; Denecke, M. A.; Jalilehvand, F.; Sandström, M.; Grenthe, I. *Inorg. Chem.* **1999**, *38*, 1795–1799.
(28) Hennig, C.; Schmeide, K.; Brendler, V.; Moll, H.; Tsushima, S.; Scheinost, A. C. *Inorg. Chem.* **2007**, *46*, 5882–5892.

indicator of the actinyl (AnO_2^{n+}) unit. Relatively large peaks at around $R + \Delta = 1.9$ Å and small but sufficiently distinguishable peaks at $R + \Delta = 2.9$ Å are attributed to the SS of the O atoms of water molecules in the uranyl equatorial plane [$O_{eq}(H_2O)$] and the MS of O_{ax}, respectively. The sharp peaks observed at $R + \Delta = 1.6-1.7$ Å are the *side lobe* peaks, which are accompanied by the strong signals of the O_{ax} shells. They are meaningless from the chemical point of view and occur as a consequence of the limited k range for the Fourier transformation.[11d,28−30] The curve-fitting results reveal that the Np^V ion is coordinated by 5.2 water molecules at 2.49 Å on its equatorial plane, whereas the Np^{VI} ion possesses 5.3 water molecules with a shorter interatomic distance of 2.42 Å. The very recent high-energy X-ray scattering study by Skanthakumar and his co-workers[11j] has suggested the presence of a Np−Np interaction with an interatomic distance of 4.2 Å in concentrated Np^V and Np^{VI} solutions ([Np] = 0.4 M). The FTs of Np^V and Np^{VI} in Figure 3 display small peaks at $R + \Delta = 3.7-3.8$ Å, which might correspond to the Np−Np interaction. These peaks are, however, so close to the noise level that their reasonable assignment is not possible.

The hydration number of actinide aquo complexes is still a matter of discussion. With regard to the spherically coordinated An ions with lower oxidation states (i.e., An^{3+} and An^{4+}), EXAFS studies have provided various hydration numbers from 9 to 11 for Th^{IV},[27] U^{IV},[27,28] Np^{III},[11g] Np^{IV},[11b,g] Pu^{III},[11b,31] Am^{III},[31] and Cm^{III} ions.[31a] Recent X-ray scattering studies by the research group of Argonne National Laboratory has demonstrated that Th^{IV} ions form a 10-coordinate hydrate complex of $[Th^{IV}(H_2O)_{10}]^{4+}$ in aqueous solution,[32] while Cm^{III} ions are coordinated by 9 water molecules to form $[Cm^{III}(H_2O)_9]^{3+}$.[33] This decrease in the hydration number with an increase in the atomic number is explicated by the actinide contraction.[34] Considering the fact that $_{93}Np$ takes a middle position between $_{90}Th$ and $_{96}Cm$ in the periodic table, Np^{III} and Np^{IV} ions are likely to have hydration numbers between 9 and 10. The observed N of 10.4 for Np^{IV} is well consistent with this hypothesis within the error limit. In the present study, EXAFS curve fitting is performed with a constant S_0^2 value of 0.9. This S_0^2 value, however, has an influence on N; that is, the larger the S_0^2 value becomes, the smaller the N value is calculated. Hence, another curve fitting was performed with $S_0^2 = 1.0$, providing $N = 9.7$. This value is still close to 10, rather than 9. These facts suggest that the 10-coordinate complex of $[Np^{IV}(H_2O)_{10}]^{4+}$ is more probable than the 9-coordinate one, $[Np^{IV}(H_2O)_9]^{4+}$. There is an agreement in the reported EXAFS[11d,g] and NMR[35] results that Np^{VI} ions (i.e., NpO_2^{2+}) are hydrated by five water molecules on its equatorial plane, forming a neptunyl(VI) pentaaquo complex of $[Np^{VI}O_2(H_2O)_5]^{2+}$. The EXAFS structural parameters obtained in this study are consistent with those previous investigations. As a matter of fact, it has been confirmed by X-ray scattering,[36] EXAFS,[11b] and NMR[35,36a] that the analogous An^{VI} ion of UO_2^{2+} forms a pentaaquo complex of $[U^{VI}O_2(H_2O)_5]^{2+}$. Besides, the density functional theory study by Spencer et al.[37] has suggested that the chemical counterparts of UO_2^{2+} and PuO_2^{2+} prefer to have the same hydration number of 5, also being supported by the NMR study.[35] Taking these facts into account, it is probably safe to conclude that $[Np^{VI}O_2(H_2O)_5]^{2+}$ is the dominant structure of the neptunyl(VI) aquo complex. The obtained $Np^{VI}-O_{ax}$ and $-O_{eq}(H_2O)$ distances (1.76 and 2.42 Å, respectively) are close to the corresponding distances for the reported uranyl(VI) and plutonyl(VI) aquo complexes determined by EXAFS: $R(U-O_{ax}) = 1.76-1.77$ Å and $R[U-O_{eq}(H_2O)] = 2.41$ Å for U^{VI},[11b,26b,28,38] and $R(Pu-O_{ax}) = 1.74$ Å and $R[Pu-O_{eq}(H_2O)] = 2.40$ Å for Pu^{VI},[39] respectively. This means that the aquo complexes of these An^{VI} ions are structurally very similar and, consequently, their behavior in practical chemical processes is supposed to be quite analogous. On the other hand, the hydration number of An^V ions is still a matter of argument. Two hydration numbers of 4[11d] and 5[11a,b,g,h] have been reported for the Np^V ion (i.e., NpO_2^{2+}), while the plutonyl(V) aquo species has been identified as a tetraaquo complex.[39] The present EXAFS result proposes the presence of the pentaaquo complex, $[Np^VO_2(H_2O)_5]^+$. However, EXAFS always suffers from relatively large errors (±10%, in this study) for the obtained coordination numbers (N). Therefore, additional EXAFS data analysis has been carried out for the Np^V spectrum by fixing $N[O_{eq}(H_2O)]$ at 3, 4, 5, and 6 and comparing the fitting residuals of each curve fit. The results are summarized in Figure 4. The fitting residual becomes smaller with increasing $N[O_{eq}(H_2O)]$, showing a minimum between $N[O_{eq}(H_2O)] = 5$ and 6. This implies that the hydration number of the Np^V ion is more likely to be larger than 5. Naturally, the Debye−Waller factor (σ^2) increases systematically with increasing $N[O_{eq}(H_2O)]$, although they are still within the appropriate values. Furthermore, the curve fitting for the EXAFS spectrum that is reproduced from the $O_{eq}(H_2O)$ peak for Np^V by performing inverse Fourier transformation from $R + \Delta = 1.8$ to 2.4 Å in Figure 3 provides a $N[O_{eq}(H_2O)]$ of 5.5 with $R(Np-O_{eq}(H_2O) = 2.49$ Å (see Figure S11 in the Supporting Information).

(29) Moll, H.; Reich, T.; Hennig, C.; Rossberg, A.; Szabó, Z.; Grenthe, I. *Radiochim. Acta* **2000**, *88*, 559–566.

(30) Ikeda, A.; Hennig, C.; Tsushima, S.; Takao, K.; Ikeda, Y.; Scheinost, A. C.; Bernhard, G. *Inorg. Chem.* **2007**, *46*, 4212–4219.

(31) (a) Allen, P. G.; Bucher, J. J.; Shuh, D. K.; Edelstein, N. M.; Craig, I. *Inorg. Chem.* **2000**, *39*, 595–601. (b) Stumpf, T.; Hennig, C.; Bauer, A.; Denecke, M. A.; Fanghänel, T. *Radiochim. Acta* **2004**, *92*, 133–138.

(32) Wilson, R. E.; Skanthakumar, S.; Burns, P. C.; Soderholm, L. *Angew. Chem., Int. Ed.* **2007**, *46*, 8043–8045.

(33) Skanthakumar, S.; Antonio, M. R.; Wilson, R. E.; Soderholm, L. *Inorg. Chem.* **2007**, *46*, 3485–3491.

(34) Katz, J. J.; Seaborg, G. T.; Morss, L. R. *Chemistry of the Actinide Elements*, 2nd ed.; Chapman and Hall: New York, 1986.

(35) Bardin, N.; Rubini, P.; Madic, C. *Radiochim. Acta* **1998**, *83*, 189–194.

(36) (a) Åberg, M.; Ferri, D.; Glaser, J.; Grenthe, I. *Inorg. Chem.* **1983**, *22*, 3986–3989. (b) Neuefeind, J.; Soderholm, L.; Skanthakumar, S. *J. Phys. Chem. A* **2004**, *108*, 2733–2739.

(37) Spencer, S.; Gagliardi, L.; Handy, N. C.; Ioannou, A. G.; Skylaris, C.-K.; Willetts, A. *J. Phys. Chem. A* **1999**, *103*, 1831–1837.

(38) Ikeda-Ohno, A.; Hennig, C.; Rossberg, A.; Tsushima, S.; Scheinost, A. C.; Bernhard, G. *Eur. J. Inorg. Chem.* **2008**, . submitted for publication.

(39) Conradson, S. D. *Appl. Spectrosc.* **1998**, *52*, 252A–279A.

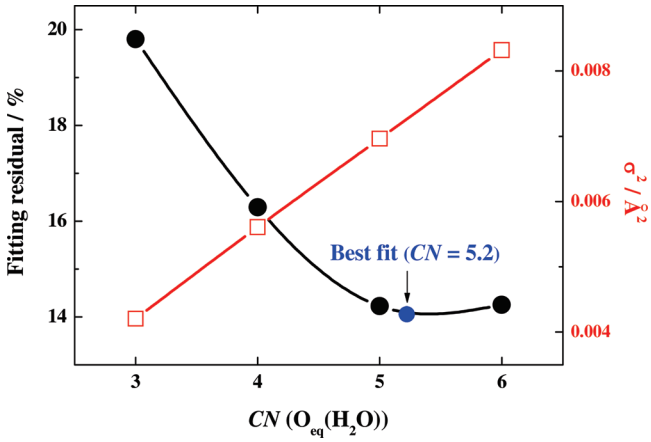

Figure 4. Variation of EXAFS fitting parameters for the neptunyl(V) aquo complex at different $N[O_{eq}(H_2O)]$ values.

In order to support the EXAFS results for Np^V, we apply the bond valence model,[40] which is based on Pauling's "2nd rule"[41] and describes the correlation between the chemical bond length (R) and the bond valence (s [vu]) with the following equation:

$$s_{ij} = \exp[(R_{ij}^0 - R_{ij})/B] \quad (3)$$

where s_{ij} and R_{ij} are the bond valence and the bond distance between i and j atoms, respectively. R_{ij}^0 is called the bond valence parameter and is obtained through a systematic analysis of relevant crystal structure data.[42] B is an empirically determined parameter. Zachariasen has defined the B value for An−O bonds as 0.35 when $s_{An-O} \leq 1$, or $B = 0.35 + 0.12(s - 1)$ when $s_{An-O} > 1$.[43] As will be mentioned below, An−$O_{eq}(H_2O)$ bonds have s values of less than 1 and, consequently, a constant value of 0.35 is employed for B in this study. The bond valence sum (V) of a given i atom is defined by using eq 3 as follows:

$$V_i = \sum_{j=1}^{N} \exp[(R_{ij}^0 - R_{ij})/B] \quad (4)$$

where N is a coordination number of the i atom. In case there is only a single type of coordinating atom (j) around the center atom of i, eq 4 can be simplified as follows:

$$V_i = N\exp[(R_{ij}^0 - R_{ij})/B] \quad (5)$$

Therefore, the coordination number N of simple single-shell complexes, such as pure aquo complexes, can be calculated from R_{ij} and V_i by using the following equation:

$$N = V_i/\exp[(R_{ij}^0 - R_{ij})/B] \quad (6)$$

The bond valence model has been utilized for characterizing a variety of solid compounds, including actinide compounds,[44] but not yet applied to solution species. Hence, we first apply this model for estimating the hydration number of the U^{VI} ion, which has already been well investigated and is generally accepted to be 5, in order to evaluate the validity of the bond valence model for solution species. The results are summarized in Table 3. According to the formal charge, the V value for the U^{VI} atom in the uranyl(VI) ion is 2.0 vu [i.e., 6 vu (U^{VI}) − 2 × 2.0 vu (O_{ax}) = 2.0 vu]. However, a recent comprehensive article by Burns and Klingensmith[45] has suggested that the axial O atoms of the uranyl(VI) ion provide only 1.9 vu on the $U^{VI}-O_{ax}$ bonding, in case the axial O atoms receive a hydrogen bond from the outer coordination sphere. This results in $V_U = 2.2$ vu for the center U^{VI} atom [i.e., 6 vu (U^{VI}) − 2 × 1.9 vu (O_{ax}) = 2.2 vu]. In fact, several studies[30,46] have implied the presence of "apical" water molecules on the axial O atoms of An ions in aqueous solution. Therefore, the N values were calculated according to the two V values of 2.0 and 2.2 vu, in order to assume the presence and absence of the apical water molecules. The estimated hydration numbers are 5.1 and 5.6 for $V_U = 2.0$ and 2.2 vu, respectively, being closed to the accepted number of 5. Consequently, we can conclude that the bond valence model is sufficiently applicable also for solution species and, hence, it is worth applying to the Np^V system. Burns and Klingensmith have also suggested in the above-mentioned article[45] that, although the V_{Np} value in the neptunyl(V) ion is formally 1.0 vu [i.e., 5 vu (Np^V) − 2 × 2.0 vu (O_{ax}) = 1.0 vu], the bond valence of the Np^V-O_{ax} bonding possesses 1.7 vu in the presence of the apical water molecules on the axial O atoms, with the result that the center Np^V atom holds 1.6 vu [i.e., 5 vu (Np^V) − 2 × 1.7 vu (O_{ax}) = 1.6 vu]. Therefore, the bond valence analysis was carried out for V_{Np} = 1.0 and 1.6 vu. Two different $R[Np^V-O_{eq}(H_2O)]$ values of 2.48 and 2.49 Å were taken into account, for considering the error in the EXAFS results. The estimated hydration number of the Np^V ion is approximately 4 when V_{Np} was assumed to be 1.0 vu, while it is close to 6 when $V_{Np} = 1.6$ vu was assumed. Considering the fact that the V_{Np} value of 1.6 vu probably reflects the actual chemical environment of the Np^V ion in aqueous solution more properly, the latter hydration number of ~6 is more trusted on the present bond valence sum analysis. Furthermore, a systematic survey of the reported crystal structures of neptunyl(V) compounds indicates that a typical $Np-O_{eq}$ distance is 2.46 Å for neptunyl(V) pentagonal complexes with $N_{eq} = 5$ and 2.55 Å for the hexagonal ones with $N_{eq} = 6$ (see Table S2 in the Supporting Information). The obtained $R[Np^V-O_{eq}(H_2O)]$ value of 2.49 Å is in the middle of these average values but slightly close to the value for the pentagonal complexes. Taking these facts into consideration, we propose that the hydration number of the Np^V ion is between 5 and 6 rather

(40) Brown, I. D. *Chem. Soc. Rev.* **1978**, *7*, 359–376.
(41) Pauling, L. *J. Am. Chem. Soc.* **1929**, *51*, 1010–1026.
(42) (a) Altermatt, D.; Brown, I. D. *Acta Crystallogr.* **1985**, *B41*, 240–244. (b) Brown, I. D.; Altermatt, D. *Acta Crystallogr.* **1985**, *B41*, 244–247.
(43) Zachariasen, W. H. *J. Less-Common Met.* **1978**, *62*, 1–7.
(44) (a) Burns, P. C.; Ewing, R. C.; Miller, M. L. *J. Nucl. Mater.* **1997**, *245*, 1–9. (b) Burns, P. C. *Can. Mineral.* **2001**, *39*, 1139–1146. (c) Van den Berghe, S.; Verwerft, M.; Laval, J.-P.; Gaudreau, B.; Allen, P. G.; Van Wyngarden, A. *J. Solid State Chem.* **2002**, *166*, 320–329. (d) Albrecht-Schmitt, T. E.; Almond, P. M.; Sykora, R. E. *Inorg. Chem.* **2003**, *42*, 3788–3795.
(45) Burns, P. C.; Klingensmith, A. L. *Elements* **2006**, *2*, 351–356.
(46) Tsushima, S.; Wahlgren, U.; Grenthe, I. *J. Phys. Chem. A* **2006**, *110*, 9175–9182.

Table 2. Summary of EXAFS Structural Parameters for Np Species in Aqueous Perchlorate and Nitrate Solutions

oxidation state of Np	medium	$O(H_2O)$		$O_{co}(NO_3)$		$N(NO_3)$		$O_{dist}(NO_3)$, MS[c]		ID[d]
		N[a]	R/Å[b]	N[a]	R/Å[b]	N[a]	R/Å[b]	N[a]	R/Å[b]	
IV	$[HClO_4] = 1.0$ M	10.4	2.40							1
	$[NO_3^-] = 5.0$ M	7.0	2.40	4.5	2.52	2.3	2.96	2.3	4.21	4
	$[NO_3^-] = 10.4$ M	5.2	2.39	6.3	2.51	3.2	2.96	3.2	4.21	7

		O_{ax}		$O_{eq}(H_2O)$		$O_{eq\text{-}co}(NO_3)$		$N(NO_3)$		$O_{dist}(NO_3)$, MS[c]		
		N[a,e]	R/Å[b]	N[a]	R/Å[b]	N[a]	R/Å[b]	N[a]	R/Å[b]	N[a]	R/Å[b]	
V	$[HClO_4] = 1.0$ M	2.0	1.84	5.2	2.49							2
	$[NO_3^-] = 5.0$ M	2.0	1.83	4	2.48	1.4	2.60	0.7	3.12	0.7	4.22	5
VI	$[HClO_4] = 1.0$ M	2.0	1.76	5.3	2.42							3
	$[NO_3^-] = 5.0$ M	2.0	1.77	4.0	2.41	1.6	2.52	0.8	2.98	0.8	4.19	6
	$[NO_3^-] = 10.4$ M	2.0	1.77	3.1	2.42	2.4	2.53	1.2	3.00	1.2	4.19	8
	$[NO_3^-] = 14.5$ M	2.0	1.76	2.4	2.43	3.9	2.52	2.0	2.98	2.0	4.19	9

[a] Error: $R \leq \pm 0.01$ Å. [b] Error: $N \leq \pm 10\%$. [c] The MS path corresponding to the linear Np−N−O_{dist} arrangement. See the text. [d] Corresponding to the ID in Table 1. [e] Fixed values. Detailed parameters are given in the Supporting Information.

Table 3. Summary of Bond Valence Sum Analysis for Uranyl(VI) and Neptunyl(V) Aquo Complexes[a]

center cation	R[An−O_{eq} (H_2O)]/Å	B	s[An−O_{eq}(H_2O)]/νu	N	
				$V_{An} = 2.0$	$V_{An} = 2.2$
UO_2^{2+}	2.41	0.35	0.393	5.1	5.6

center cation	R[An−O_{eq} (H_2O)]/Å	B	s[An−O_{eq}(H_2O)]/νu	N	
				$V_{An} = 1.0$	$V_{An} = 1.6$
NpO_2^+	2.48	0.35	0.281	3.6	5.7
	2.49	0.35	0.273	3.7	5.8

[a] R[An−O_{eq} (H_2O)]^0 was set to be 2.083 Å for U^{VI} and 2.036 Å for Np^V, respectively, according to refs 43 and 44d.

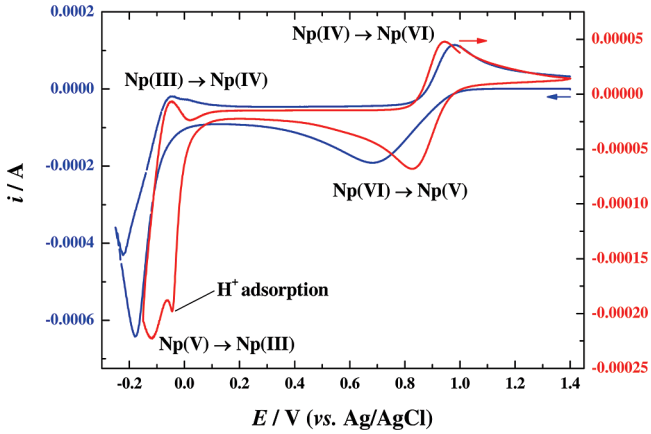

Figure 5. CVs of 0.04 M Np^{VI} in HNO_3/NH_4NO_3 solutions using Pt electrode: blue line, 1.0 M HNO_3/4.0 M NH_4NO_3 (initial scan direction = cathodic from 1.4 V); red line, 4.4 M HNO_3/6.0 M NH_4NO_3 (initial scan direction = anodic from 1.0 V); scan rate, 400 mV/s.

than 4. The actual neptunyl(V) aquo complex may be a mixture of $[Np^VO_2(H_2O)_5]^+$ and $[Np^VO_2(H_2O)_6]^+$. Besides, a recent high-energy X-ray scattering study by Skanthakumar and his co-workers[11j] has suggested that Np^V and Np^{VI} ions are surrounded by five water molecules on their equatorial planes, being well consistent with our results.

Nitrate System. Cyclic voltammetry of Np^{VI} was carried out in 5.0 and 10.4 M nitrate solutions to investigate its redox behavior. The obtained CVs are given in Figure 5 and in Figures S1 and S2 in the Supporting Information. Although the redox potentials are slightly shifted, the electrochemical behavior of Np^{VI} in the nitrate system is essentially the same as that in the previous perchlorate system: the two peaks corresponding to the reduction from Np^{VI} to Np^V and from Np^V to Np^{III} are observed on the cathodic scan, while there are also two distinguishable peaks, which are attributed to the oxidation from Np^{III} to Np^{IV} and that from Np^{IV} to Np^{VI}, respectively, on the anodic scan. This voltammetric behavior is consistent with the reported CVs for Np in HNO_3.[8b,d] A detailed data analysis was performed for the CVs of a Np^{VI}/Np^V redox couple (Figures S1 and S2 in the Supporting Information) to evaluate their electrochemical parameters. The CV simulations by assuming a quasi-reversible reaction suggest that the formal potential, E^0, was decreased from 0.91 to 0.89 V as the nitrate concentration was increased from 5.0 to 10.4 M. To the contrary, the kinetic parameters of k^0_{norm} and α increase from 0.13 ± 0.10 to 0.32 ± 0.10 and from 0.32 ± 0.03 to 0.42 ± 0.02, respectively, with an increase in the nitrate concentration. This indicates that the redox reaction of the Np^{VI}/Np^V couple becomes faster and its energy barrier gets closer to symmetry ($\alpha = 0.5$) with an increase in the nitrate concentration. The sharp peak observed at 0 V in the CV for the 10.4 M nitrate solution became more intense with an increase in the HNO_3 concentration. This peak is related to the adsorption of H^+ on the surface of the Pt electrode, and it completely hinders the following reduction peak to Np^{III} in more than 6 M HNO_3. Therefore, the reduction potential for preparing Np^{III}/Np^{IV} cannot be estimated in nitrate solutions having more than 6 M HNO_3.

According to the redox potentials observed in the CVs, the oxidation state of Np was adjusted in different nitrate concentrations by bulk electrolysis. Detailed conditions of the electrolysis are summarized in Table 1. The reduction of Np^{VI} at 0.2 V produced a blue-green solution of Np^V in any nitrate concentration. However, the Np^V species prepared in the nitrate solution containing more than 5 M HNO_3 were

gradually reoxidized to Np^{VI} by nitrous acid (HNO_2),[47] which is produced in a higher concentration of HNO_3. Adding hydrazine (N_2H_4) into the solution restrains the production of HNO_2.[48] However, N_2H_4 is a strong reductant and it reduces Np^{VI}/Np^{V} to Np^{IV}. Additionally, the following disproportionation reaction of Np^{V} is promoted with an increase in the acid concentration.[49]

$$2Np^{V}O_2^{+} + 4H^{+} \leftrightarrow Np^{4+} + Np^{VI}O_2^{2+} + 2H_2O$$

As a consequence, only one neptunium(V) nitrate sample was prepared in a mixed nitrate solution of 1.0 M HNO_3/4.0 M NH_4NO_3, and no further pure Np^{V} sample could be electrochemically prepared in a higher HNO_3 concentration. Another electrolysis was carried out at −0.3 V to prepare Np^{IV} samples. As was observed in the previous perchlorate system, the reduction of Np^{VI} at −0.3 V produced a dark-brown solution of Np^{III}, and the obtained Np^{III} was immediately oxidized to Np^{IV} in air. However, the electrolysis performed with the solution containing more than 6 M HNO_3 only resulted in gas production (probably H_2) on the working electrode, and no reduction reaction to Np^{III} or Np^{IV} proceeded regardless of the duration time of the electrolysis. As a result, pure Np^{IV} samples could be prepared in 1.0 M HNO_3/4.0 M NH_4NO_3 and in 4.4 M HNO_3/6.0 M NH_4NO_3. In addition to these one Np^{V} and two Np^{IV} samples, three Np^{VI} samples were prepared in different nitrate concentrations. The prepared neptunium(VI) nitrate solution had a pale-ocher color, which is different from the purple color observed for the neptunium(VI) perchlorate solution. The UV−visible absorption spectra of these neptunium nitrate samples are shown in Figure 6 and in Figures S4 and S5 in the Supporting Information. The spectra in 1.0 M HNO_3/4.0 M NH_4NO_3 are not identical with those in the perchlorate solution but are quite similar to the reported spectra in 4.0 M HNO_3.[10a] A clear systematic change is observed on the Np^{VI} spectra in Figure 6. That is, the intense peak at 1225 nm weakens and, instead, a new peak arises at 1120 nm according to an increase in the nitrate concentration. Besides, there is a remarkable change in the fine structures observed in the region from 400 to 700 nm. These spectral changes suggest the presence of inner-sphere complexation between the Np^{VI} ion and the nitrate ion (NO_3^{-}).

Figures 7−9 represent the k^3-weighted Np L_{III}-edge EXAFS spectra (left) and their corresponding FTs (right) for Np^{IV}, Np^{V}, and Np^{VI} in the aqueous nitrate solutions, along with those in 1.0 M $HClO_4$. The [2p4f] double-electron excitation[11i] feature, which has been observed at k = 10.7 Å^{-1} in the k-range spectra in the perchlorate system, is clearly distinguishable in each nitrate concentration for the Np^{IV} and Np^{VI} spectra, while it is almost hidden by the EXAFS oscillation on the Np^{V} spectra. Although both the EXAFS spectra and the FTs show clear spectral changes for all of the oxidation states according to an increase in the nitrate concentration, the FTs exhibit

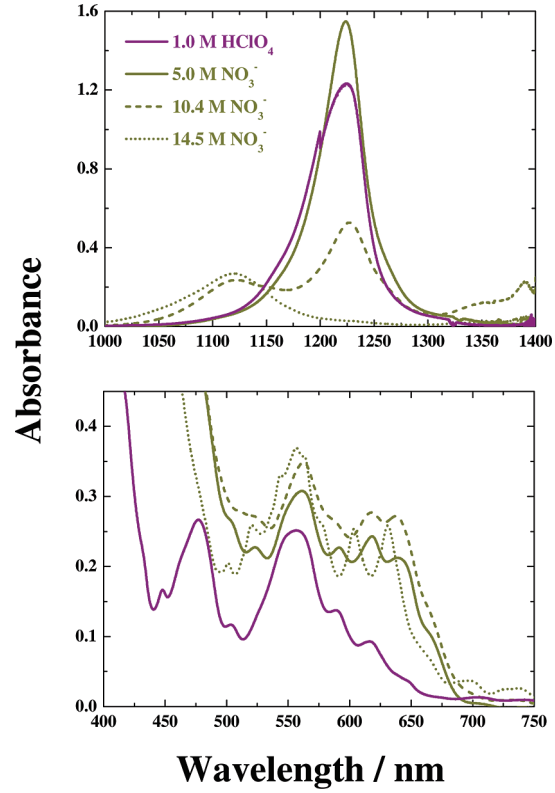

Figure 6. UV−visible absorption spectra of Np^{VI} in aqueous perchlorate and nitrate solutions: [Np^{VI}] = 0.04 M; optical path length = 1.0 cm; solvent compositions, "5.0 M NO_3^{-}" = 1.0 M HNO_3/4.0 M NH_4NO_3, "10.4 M NO_3^{-}" = 4.4 M HNO_3/6.0 M NH_4NO_3, and "14.5 M NO_3^{-}" = 14.5 M HNO_3. The data color reflects the actual color of the sample solutions.

more systematic changes. That is, in addition to the O peaks of hydrated water molecules at $R + \Delta$ = 1.9−2.0 Å (and the O_{ax} peaks for Np^{V} and Np^{VI}), two additional peaks grow on the Np^{IV} and Np^{V} spectra at $R + \Delta$ = 2.5 and 3.6 Å for Np^{IV} and 2.1 and 3.6 Å for Np^{V}, respectively, upon an increase in the nitrate concentration. Besides, three additional peaks rise at $R + \Delta$ = 2.0, 2.6, and 3.7 Å on the Np^{VI} spectra, with an increase in the nitrate concentration. A similar systematic change has also been observed for the homologous An^{IV} and An^{VI} of Pu^{IV} [50] and U^{VI} [38] in HNO_3. It has been reported that the nitrate ion prefers to coordinate to An ions in a bidentate fashion in solution rather than in a unidentate one.[38,50−52] Therefore, the curve fitting was performed by assuming the bidentate mode for the coordinating nitrate ions. A possible coordination geometry of uni- and bidentate nitrate ions to the neptunyl ion [i.e., $NpO_2NO_3(aq)$] is illustrated in Figure S26 in the Supporting Information. The growing FT peaks observed at $R + \Delta$ = 2.0−2.1, 2.5−2.6, and 3.6−3.7 Å are attributed to the SS paths of the coordinating O atoms (O_{co}), N atoms (N), and distal O atoms (O_{dist}) of nitrate ions, respectively. The distances between these three shells are well consistent with the

(47) Siddall, T. H.; Dukes, E. K. *J. Am. Chem. Soc.* **1959**, *81*, 790–794.
(48) Biddle, P.; Miles, J. H. *J. Inorg. Nucl. Chem.* **1968**, *30*, 1291–1297.
(49) Keller, C. *The Chemistry of the Transuranium Elements*; VCH: Weinheim, Germany, 1971.
(50) Allen, P. G.; Veirs, D. K.; Conradson, S. D.; Smith, C. A.; Marsh, S. F. *Inorg. Chem.* **1996**, *35*, 2841–2845.
(51) Gaillard, C.; Chaumont, A.; Billard, I.; Hennig, C.; Quadi, A.; Wipff, G. *Inorg. Chem.* **2007**, *46*, 4815–4826.
(52) Ikeda, A.; Hennig, C.; Rossberg, A.; Tsushima, S.; Scheinost, A. C.; Bernhard, G. *Anal. Chem.* **2008**, *80*, 1102–1110.

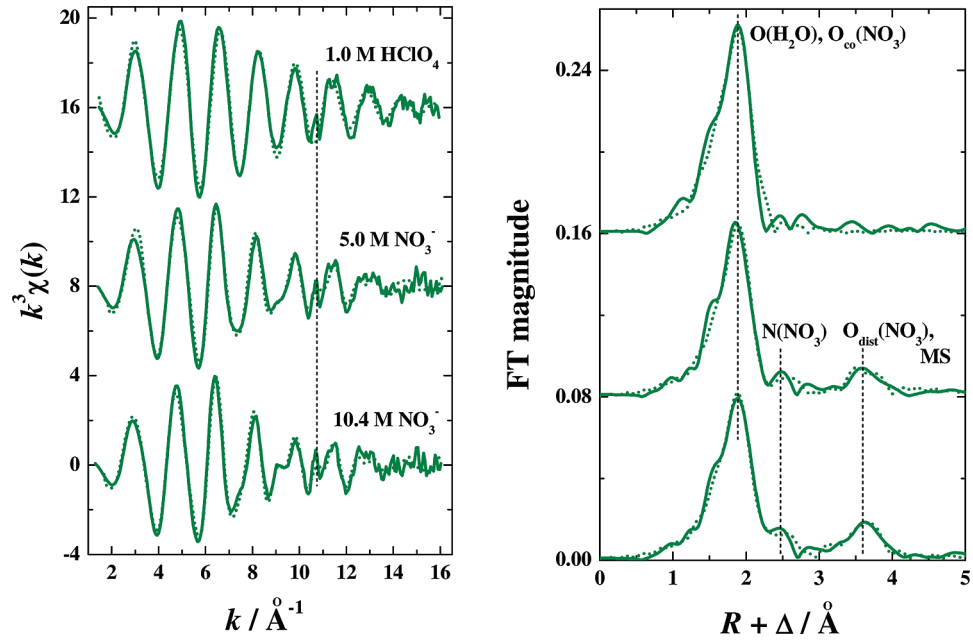

Figure 7. k^3-weighted Np L_{III}-edge EXAFS spectra (left) and their corresponding FTs (right) for Np^{IV} in aqueous perchlorate and nitrate solutions: —, experimental data; •••, theoretical fit; FT range, $k = 1.5-16.0$ Å^{-1}; phase shifts are not corrected on the FTs; solvent compositions, "5.0 M NO_3^-" = 1.0 M HNO_3/4.0 M NH_4NO_3 and "10.4 M NO_3^-" = 4.4 M HNO_3/6.0 M NH_4NO_3. The data color reflects the actual color of the sample solutions. The dotted line on the EXAFS spectra represents the [2p4f] double-electron excitation. See the text.

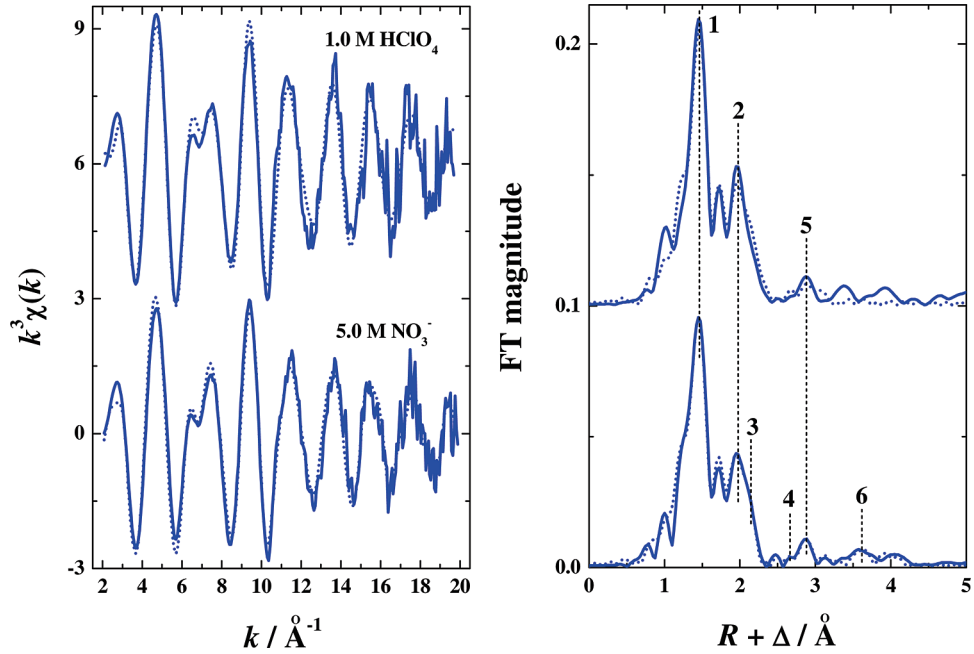

Figure 8. k^3-weighted Np L_{III}-edge EXAFS spectra (left) and their corresponding FTs (right) for Np^V in aqueous perchlorate and nitrate solutions: —, experimental data; •••, theoretical fit; FT range, $k = 2.0-19.5$ Å^{-1}; phase shifts are not corrected on the FTs; solvent compositions, "5.0 M NO_3^-" = 1.0 M HNO_3/4.0 M NH_4NO_3; numbers of FT peaks, 1 = O_{ax}, 2 = $O_{eq}(H_2O)$, 3 = $O_{eq\text{-}co}(NO_3)$, 4 = N, 5 = O_{ax} MS, 6 = $O_{dist}(NO_3)$ and its MS, The data color reflects the actual color of the sample solutions.

bidentate coordination[38,50−52] rather than the unidentate one. Besides, it is well-known[38,50−52] that the bidentate-coordinating nitrate ions produce an enhanced MS peak[17] at the same distance where the O_{dist} peak is observed because of the linear arrangement of metal−N−O_{dist}. In fact, the magnitude of the O_{dist} peak at $R + \Delta = 3.6-3.7$ Å is considerably larger, in spite of its longer distance from the absorbing Np atom. Considering these facts, we conclude that the bidentate mode is a dominant coordination mode between Np ions and NO_3^- in aqueous solution for all of the oxidation states.

The structural parameters obtained from the curve fitting are summarized in Table 2. Thermodynamic data[5] have suggested that there are four species of mono-, di-, tri-, and tetranitrato complexes formed in an aqueous nitrate solution for the Np^{IV} system, while only two possible species of mono- and dinitrato complexes are identified in the Np^V and Np^{VI} systems. On the other hand, the reported EXAFS studies

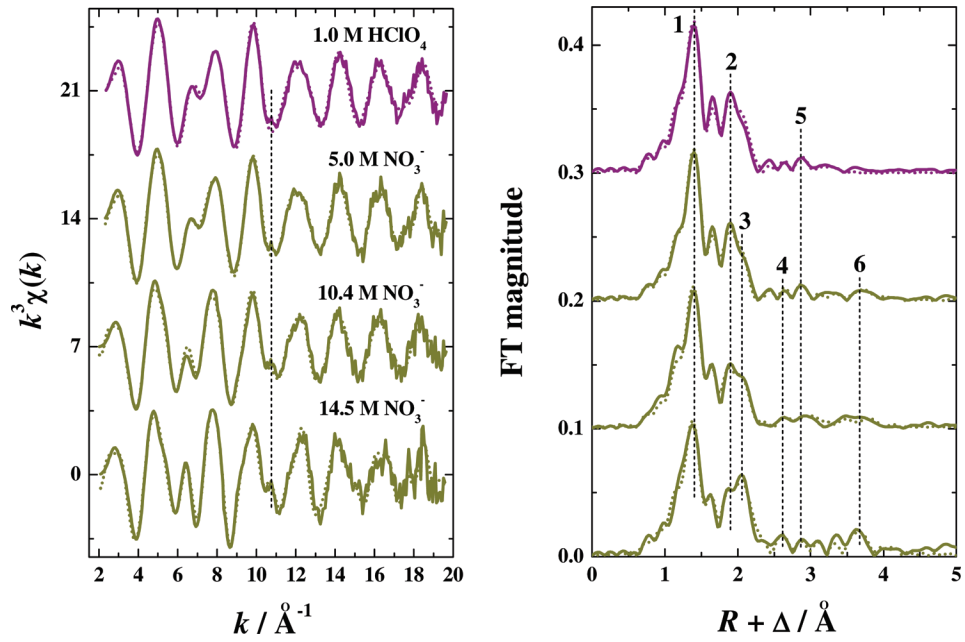

Figure 9. k^3-weighted Np L_{III}-edge EXAFS spectra (left) and their corresponding FTs (right) for Np^{VI} in aqueous perchlorate and nitrate solutions: —, experimental data; •••, theoretical fit; FT range, $k = 2.0-19.5$ Å^{-1}; phase shifts are not corrected on the FTs; solvent compositions, "5.0 M NO_3^-" = 1.0 M HNO_3/4.0 M NH_4NO_3, "10.4 M NO_3^-" = 4.4 M HNO_3/6.0 M NH_4NO_3, and "14.5 M NO_3^-" = 14.5 M HNO_3; numbers of FT peaks, 1 = O_{ax}, 2 = $O_{eq}(H_2O)$, 3 = $O_{eq\text{-}co}(NO_3)$, 4 = N, 5 = O_{ax} MS, 6 = $O_{dist}(NO_3)$ and its MS. The data color reflects the actual color of the sample solutions. The dotted line on the EXAFS spectra represents the [2p4f] double-electron excitation. See the text.

performed in high ionic strength media have revealed that Pu^{IV} ions form a hexanitrato complex of $[Pu(NO_3)_6]^{2-}$ in 13 M HNO_3,[50] while U^{VI} ions are surrounded by nearly three nitrate ions in 14.5 M HNO_3, possibly forming a trinitrato complex of $[UO_2(NO_3)_3]^-$.[38] The present EXAFS results indicate that the hydrated water molecules in the primary coordination sphere of Np are replaced by bidentate coordinate nitrate ions according to an increase in the nitrate concentration. As a result, Np^{IV} ions are coordinated by 3.2 nitrate ions in 10.4 M NO_3^- solution on average. The speciation distribution estimated from the reported formation constants[6a,d] suggests that a tetranitratoneptunium(IV) complex of $[Np(H_2O)_m(NO_3)_4]^0$ is dominant in a 10 M NO_3^- solution, coexisting with a slight amount of the trinitrato species (see Figures S27 and S28 in the Supporting Information). Therefore, the calculated $N(NO_3)$ $\{=N[O_{co}(NO_3)]/2 = N[N(NO_3)]\}$ of 3.2 probably represents the coexistence of the tri- and tetranitratoneptunium(IV) complexes in the present 10.4 M NO_3^- solution. A hexanitrato complex of $[Np(NO_3)_6]^{2-}$, which is analogous to the reported hexanitratoplutonium(IV) complex, is not likely to be formed in the present nitrate concentration range. This may indicate that the nitrate complexation is weaker for Np^{4+} than for Pu^{4+}. The $Np-O_{co}(NO_3)$ distances of 2.51−2.52 Å are slightly longer than those observed in the crystal structure of $[Np(NO_3)_6]^{2-}$ [$Np-O_{co}(NO_3) = 2.50$ Å on average],[53] while the observed $Np-O_{co}(NO_3)$ distances are shorter than that for the aqueous thorium(IV) nitrate species [$Th-O_{co}(NO_3) = 2.63$ Å][54] but longer than that for the plutonium(IV) nitrate species [$Pu-O_{co}(NO_3) = 2.49$ Å].[50] This may indicate the presence of the actinide contraction also in the $An^{IV}-NO_3$ complexation, as has been observed in the trivalent lanthanide (Ln^{III}) nitrate complexes in aqueous solution.[55] The overall coordination number of Np^{IV} appears to increase from 10.4 to 11.5 with an increase in the nitrate concentration.

The hydrated water molecules on the equatorial plane of the Np^{VI} ion are also replaced continuously with nitrate ions by an increase in the the nitrate concentration. The present EXAFS results suggest that, on average, two nitrate ions coordinate to the Np^{VI} ion in the highest HNO_3 concentration of 14.5 M. To date, the formation constants of neptunium(VI) nitrate complexes in aqueous solution have been reported for the mono- and dinitrato complexes but not for the trinitrato complex.[5] However, the homologous An^{VI} ion of the U^{VI} ion forms the trinitrato complex in aqueous solution with a higher nitrate concentration.[38,56] Considering the fact that similar formation constants have been reported for the mono- and dinitrato complexes of U^{VI} and Np^{VI} ions,[5,56] we expect that Np^{VI} ions also form the trinitrato complex under high nitrate concentration conditions. Assuming that the speciation distribution of neptunyl(VI) nitrato complexes in aqueous solution is similar to that of uranyl(VI) nitrato complexes, Np^{VI} ions are supposed to exist as a mixture of mono-, di-, and trinitrato complexes even in 14.5 M HNO_3.[38] Hence, $N(NO_3)$ of 2.0 obtained for 14.5 M HNO_3 represents the average of these three nitrate species. In the present study,

(53) (a) Grigor'ev, M. S.; Gulev, B. F.; Krot, N. N. *Radiokhimiya* **1986**, *28*, 685–690. (b) Grigor'ev, M. S.; Yanovskii, A. I.; Krot, N. N.; Struchkov, Y. T. *Radiokhimiya* **1987**, *29*, 574–579.
(54) Johansson, G.; Magini, M.; Ohtaki, H. *J. Solution Chem.* **1991**, *20*, 775–792.
(55) Yaita, T.; Narita, H.; Suzuki, S.; Tachimori, S.; Motohashi, H.; Shiwaku, H. *J. Radioanal. Nucl. Chem.* **1999**, *239*, 371–375.
(56) Grenthe, I.; Fuger, J.; Konings, R. J. M.; Lemire, R. J.; Muller, A. B.; Nguyen-Trung, C.; Wanner, H. In *Chemical Thermodynamics of Uranium*; Wanner, H., Forest, I., Eds.; OECD-NEA: Paris, 1991 (2003 updated).

we obtain the structural information of neptunium(V) nitrate species only for a 5.0 M NO_3^- solution. This is not sufficient for discussing the systematic variation in the nitrate complexation and the detailed speciation. However, the interatomic distances obtained from EXAFS are in good agreement with those in the reported crystal structures of neptunyl(V) nitrato complexes {$R(Np-O_{ax}) = 1.83-1.84$ Å, $R[Np-O_{eq}(H_2O)] = 2.48$ Å, and $R[Np-O_{eq\text{-}co}(NO_3)] = 2.59-2.61$ Å},[57] supporting the reliability of the obtained interatomic distances.

The $Np-O_{eq\text{-}co}(NO_3)$ distance lengthens from 2.52−2.53 to 2.60 Å as a result of the reduction from Np^{VI} to Np^{V}. This is mainly due to the decrease in the net charge of the Np ion. However, their coordination numbers are almost unchanged between Np^{VI} and Np^{V} in the same solution, not only for the nitrate system but also for the previous perchlorate system. This indicates that Np ions undergo no structural rearrangement through the redox reaction between Np^{VI} and Np^{V} in these two aqueous solution systems. Np^{IV} exhibits a slightly shorter $Np-O_{co}(NO_3)$ distance than Np^{VI}. Taken together, these results suggest that the $Np-O_{co}(NO_3)$ bonding becomes loosened in the following order: $Np^{IV} > Np^{VI} > Np^{V}$. The difference between $R[Np-O(H_2O)]$ and $R[Np-O_{co}(NO_3)]$ is almost constant (0.11−0.12 Å) for all of the oxidation states. Besides, the interatomic distance is left relatively unchanged for each oxidation state, regardless of the nitrate concentration.

Conclusion

Neptunium can possess three different oxidation states of IV, V, and VI in aqueous acidic solutions of $HClO_4$ and HNO_3/NH_4NO_3, although Np^{V} is not stable in the nitrate solution containing more than 5 M HNO_3. These Np species can be prepared electrochemically by using a Pt electrode. The electrochemical behavior of Np in acidic perchlorate and acidic nitrate solutions is essentially the same. The electrochemical reaction process of the Np^{VI}/Np^{V} redox couple involves no structural rearrangement, while their chemical bondings weaken and the interatomic distances between Np and coordinating atoms lengthen as a result of the reduction from Np^{VI} to Np^{V}, mainly because of the decrease in the net charge of the Np atom. The tetravalent Np ion of Np^{4+} is surrounded by 10 or 11 water molecules in $HClO_4$. These hydrate water molecules are replaced by bidentate-coordinating nitrate ions upon an increase in the nitrate concentration, finally forming the two dominant species of tri- and tetranitrato complexes, $[Np(H_2O)_l(NO_3)_3]^+$ and $[Np(H_2O)_m(NO_3)_4]^0$, in a 10 M NO_3^- solution. On the other hand, the penta- and hexavalent neptunium form the neptunyl ion, NpO_2^{n+} ($n = 1$ for Np^{V} and 2 for Np^{VI}), which is coordinated by five (or possibly six for Np^{V}) water molecules in its equatorial plane. These hydrate water molecules are also replaced by several bidentate-coordinating nitrate ions according to an increase in the nitrate concentration, with the result that the speciation of Np^{VI} is a mixture of mono-, di-, and trinitratoneptunyl(VI) complexes in 14.5 M HNO_3. The interatomic distances between Np and $O(H_2O)$ and between Np and $O_{co}(NO_3)$ are increased in the following order: $Np^{IV} < Np^{VI} < Np^{V}$. This probably indicates that the coordination of water molecules and nitrate ions in the Np primary coordination sphere becomes weaker in the same order.

Acknowledgment. We thank K. Takao for the fruitful discussion on electrochemistry. This research was supported by the Deutsche Forschungsgemeinschaft under Contract HE 2297/2-1.

Supporting Information Available: CVs in nitrate solutions, UV−visible absorption spectra, XAFS data that are not given in the text and the detailed EXAFS structural parameters, and the speciation distribution diagrams of neptunium(IV) nitrate species. This material is available free of charge via the Internet at http://pubs.acs.org.

IC8009095

(57) (a) Grigor'ev, M. S.; Charushnikova, I. A.; Krot, N. N.; Yanovskii, A. I.; Struchkov, Y. T. *Z. Neorg. Khim.* **1994**, *39*, 179–183. (b) Andreev, G. B.; Budantseva, N. A.; Antipin, M. Y.; Krot, N. N. *Russ. J. Inorg. Chem.* **2002**, *28*, 434–438.